

# Higgs Boson Production Rates in Hadronic Collisions

S. Dawson\*

*Physics Department, Brookhaven National Laboratory  
Upton, N.Y. 11973*

(Dated: November 28, 2018)

Higgs boson production rates at hadron colliders are reviewed with particular emphasis on progress in the calculation of higher order QCD effects. Emphasis is placed on the uncertainties in the predictions for Higgs boson production. A firm understanding of these uncertainties is crucial for extracting new physics signals.

## I. INTRODUCTION

The search for the Higgs boson is one of the fundamental goals of the Tevatron and the LHC. At the Tevatron, discovery relies on the observation of the Higgs signal in many channels, since the rate is quite small. In order to disentangle a Higgs boson from the background, it is crucial to have reliable predictions for both the signal and the background and to well understand the uncertainties in the theoretical predictions. The case is somewhat different at the LHC, since the Higgs boson production rate is significantly larger than at the Tevatron. Here discovery is more straightforward, and the question becomes what can we learn about the underlying physics. This again requires a firm understanding of the production rates and decay patterns.

In this paper, we review the predictions for the production of the Higgs boson in the Standard Model at the Tevatron and at the LHC. The current status of QCD radiative corrections to Higgs boson production is examined critically in order to make estimates of the uncertainties involved in the predictions. The next-to-leading order (NLO) results are now available for all of the dominant production channels and the forefront of activity has moved to the calculation of next-to-next-to-leading order (NNLO) corrections and the resummation of leading and next-to-leading order logarithmic effects. The implementation of these higher order effects in Monte Carlo programs and the comparison with fixed order perturbative calculations remains an active area of investigation.

## II. LHC

Many studies have been made of the capability of the LHC to observe the Higgs boson in a variety of channels. With  $30 \text{ fb}^{-1}$ , a Standard Model Higgs boson will be observable at the  $5\sigma$  level over the entire mass range,  $100 \text{ GeV} < M_h < 1 \text{ TeV}$ . With  $100 \text{ fb}^{-1}$ , the Higgs boson will be observable in at least 2 channels in the same mass range. By combining various channels, some measurements of Higgs couplings will then be possible. The conclusions of these studies, however, typically rely on the use of the lowest order cross sections only.[1] The NLO QCD results exist for all the relevant Higgs production and decay channels, but not for many of the backgrounds.

### A. Gluon Fusion

The dominant production mechanism for the Higgs boson at the LHC is gluon fusion. The NLO QCD corrections are well known, both in the  $M_t \rightarrow \infty$  limit and with the inclusion of the complete  $M_t$  dependence of the result.[2] A convenient parameterization of the results is given by the  $K$  factor,

$$K(\mu^2) \equiv \frac{\sigma_{NLO}(\mu^2)}{\sigma_{LO}(\mu^2)} .$$

We have explicitly included the dependence on  $\mu$  to emphasize the fact that the  $K$  factor is typically quite sensitive to the renormalization/factorization scale  $\mu$ . The  $M_t \rightarrow \infty$  limit provides an extremely accurate description of the full rate at NLO, as can be seen in Fig. 1. By including the exact  $M_h$  and  $M_t$  dependence in

---

\*dawson@bnl.gov

TABLE I:  $pp \rightarrow h$  at  $\sqrt{s} = 14$  TeV (CTEQ5, set4;  $\mu = M_h$ )

	$M_h = 100$ GeV		$M_h = 500$ GeV		$M_h = 900$ GeV	
	$\sigma_{\text{NLO}}(pb)$	$\sigma_{\text{NLO}}^\infty(pb)$	$\sigma_{\text{NLO}}(pb)$	$\sigma_{\text{NLO}}^\infty(pb)$	$\sigma_{\text{NLO}}(pb)$	$\sigma_{\text{NLO}}^\infty(pb)$
$M_b = 4$ GeV $M_t = 175$ GeV $\alpha_s(M_Z) = .118$	48.3	48.6	4.1	4.3	.23	.25
$M_b = 5$ GeV $M_t = 175$ GeV $\alpha_s(M_Z) = .118$	48.0	48.2	4.1	4.4	.23	.25
$M_b = 4$ GeV $M_t = 175$ GeV $\alpha_s(M_Z) = .120$	50.2	51.0	4.2	4.5	.24	.27
$M_b = 4$ GeV $M_t = 180$ GeV $\alpha_s(M_Z) = .118$	48.1	48.5	4.2	4.5	.25	.27

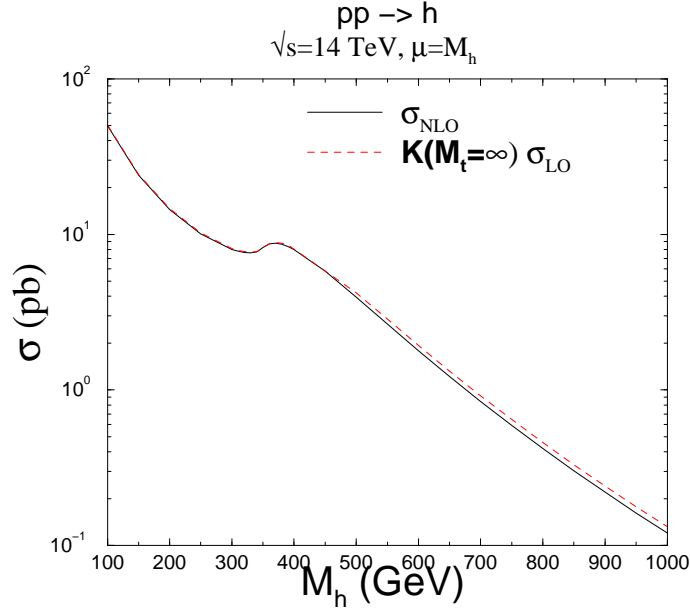


FIG. 1: Complete NLO result for inclusive Higgs boson production at the LHC,  $\sqrt{s} = 14$  TeV, with a renormalization/factorization scale  $\mu = M_h$  (solid). The dashed line is obtained by combining the complete lowest order result with the  $K$  factor computed in the limit  $M_t \rightarrow \infty$ .

the lowest order result and multiplying by the  $K$  factor computed in the  $M_t \rightarrow \infty$  limit, ( $\sigma_{m_t \rightarrow \infty}$ ), the resulting approximation to the next-to-leading order rate is extremely accurate all the way up to  $M_h \sim 1$  TeV. Table 1 shows the dependence of the NLO cross section on various input parameters. The exact NLO calculation has a small dependence on  $m_b$  through the  $b$  quark loop.

The NLO corrections to the LO rate are quite large, increasing the cross section by about a factor of 2. In addition, the scale dependence remains significant. The LHS of Fig. 2 compares the complete LO order result with the NLO result. The bands represent a variation of the renormalization scale from  $\frac{M_h}{2} < \mu < 2M_h$ . Note that there is no overlap between the bands labelled LO and NLO and so, in this case, the variation of the scale  $\mu$  appears to be a poor indicator of the uncertainty of the result.

The accuracy of the NLO  $K$  factor computed in the  $M_t \rightarrow \infty$  limit has encouraged two groups to undertake

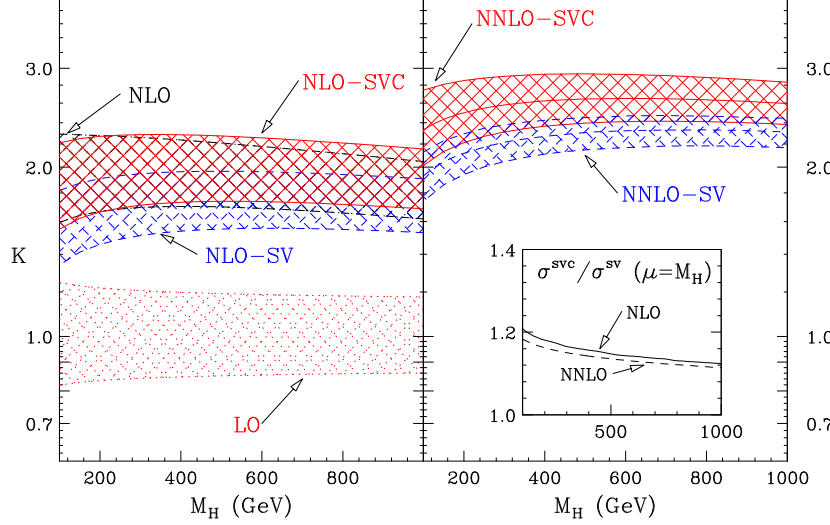


FIG. 2: The curved labelled LO (NLO) on the LHS are the lowest order (next-to-leading-order) result for  $pp \rightarrow h$  at the LHC with the renormalization scale varied from  $\frac{M_h}{2} < \mu < 2M_h$ . The curve labelled NLO-SVC on the LHS includes the terms of Eq. 1 with  $i = j = 1$ , along with the NLO virtual corrections. The curve labelled NNLO-SVC on the RHS includes the terms of Eq. 1 with  $i = 1, 2, 3$  and of Eq. 2 with  $j = 3$ , plus the NNLO virtual corrections. From Ref. [4].

the calculation of the NNLO contribution to inclusive Higgs production in this limit.[3, 4] Using an effective theory corresponding to an infinite top quark mass, the NNLO virtual corrections reduce to 2-loop Feynman diagrams, instead of the 3-loop diagrams they would be in the complete  $M_t$  dependent calculation. These virtual contributions to the NNLO rate have been computed by Harlander.[5]

At present, the existing NNLO results for the inclusive Higgs production rate are incomplete and make an assumption which the authors term the “soft approximation”. This approximation includes the leading terms as  $z \equiv M_h^2/\hat{s} \rightarrow 1$ , (where  $\sqrt{\hat{s}}$  is the gluon-gluon center of mass energy). These leading  $z \rightarrow 1$  contributions are of the form,

$$\delta(1-z), \quad \left( \frac{\log^i(1-z)}{1-z} \right)_+, \quad i = 1, 2, 3 \quad . \quad (1)$$

These terms are expected to provide the bulk of the NNLO corrections. The validity of the soft approximation can be tested at NLO by comparison with the complete calculation. Inclusion of the leading soft terms of Eq. (1) with  $i = 1$ , (the curve labelled NLO-SV of Fig. 2), shows that the soft plus virtual contributions alone underestimate the exact NLO result by  $\sim 15 - 20\%$ .

In order to obtain a more accurate approximation to the complete rate, the sub-leading collinear contributions can also be included. These terms are of the form

$$\log^j(1-z), \quad j = 1, 2, 3. \quad (2)$$

The leading collinear contributions at each order ( $j=1$  for NLO and  $j = 3$  for NNLO) have been found in Refs. [3, 4]. In addition, the sub-leading collinear contributions ( $j = 1, 2$  at NNLO) can be estimated from the resummation calculation of Ref. [6]. From Fig. 2, we see that including the collinear  $\log(1-z)$  contribution, along with the virtual contribution and the soft terms of Eq. 1 (with  $i = 1$ ), provides an excellent approximation to the full NLO result (the curve labelled NLO-SVC in Fig. 2).

Using the soft plus collinear approximation to the NNLO result,  $i = 1, 2, 3$  in Eq. (1) and  $j = 3$  in Eq. (2), yields the results shown on the RHS of Fig. 2 (labelled NNLO-SVC). We see that the NNLO corrections are large, leading to a  $K$  factor between 2.5 and 3. The bands correspond to varying the renormalization scale between  $M_h/2 < \mu < 2M_h$ . The scale dependence is only slightly reduced from that of the NLO result.

Harlander and Kilgore[3] included also the sub-leading collinear terms of the form  $\log^2(1-z)$  and  $\log(1-z)$ , to obtain the solid curves shown in Fig. 3. The differences between the 3 upper curves in Fig 3 is due taking different approximations for the unknown sub-leading collinear contributions to the NNLO result and can be

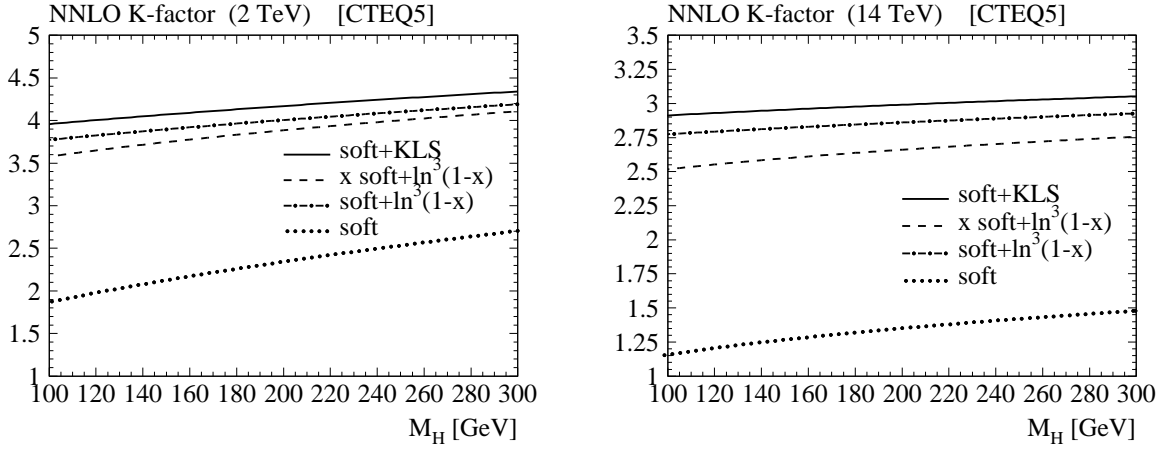


FIG. 3: (a) NNLO result for the  $K$  factor for  $p\bar{p} \rightarrow h$  at  $\sqrt{s} = 2$  TeV with  $\mu = M_h$ . (b) NNLO result for the  $K$  factor for  $pp \rightarrow h$  at  $\sqrt{s} = 14$  TeV with  $\mu = M_h$ . From Ref [3].

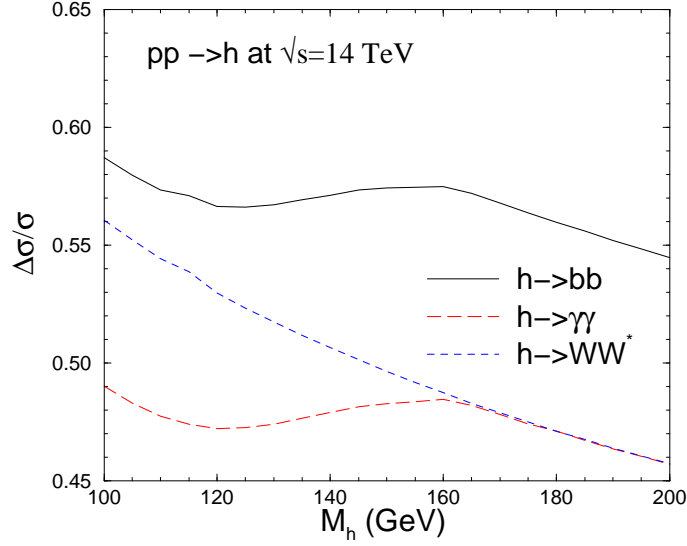


FIG. 4: Uncertainty on the production cross section times branching ratio to NLO at the LHC for various Higgs channels.  $\mu$  is varied from  $M_h/2 < \mu < 2M_h$ ,  $\alpha_s(M_Z)$  from  $.115 < \alpha_s(M_Z) < .123$  and  $m_b$  from  $4.5 \text{ GeV} < m_b(m_b) < 5 \text{ GeV}$ .

interpreted as an estimate of the uncertainty of the result. As is clear from this figure, the collinear contribution from the  $\log^j(1-z)$  terms is numerically quite large, (since the dotted curve labelled “soft” omits the  $\log^j(1-z)$  contributions). The inset in the RHS of Fig. 2 also show the importance of the collinear contributions.

Another important issue is the question of NNLO parton distribution functions (pdfs). At present only partial NNLO pdfs exist.[7] Catani *et.al.* use the NNLO pdfs of Ref. [7], while Harlander and Kilgore utilize CTEQ5 NLO pdfs. The inclusion of NNLO pdfs (instead of NLO pdfs) decreases the rate by roughly 8%.[4] Clearly a complete NNLO calculation with complete NNLO pdfs is needed before we can begin to extract precision results. At present, the best estimate is that there is still approximately a 35% uncertainty in the prediction due to scale dependence, unknown NNLO terms, incomplete knowledge of the NNLO pdfs, and our knowledge of  $\alpha_s$ .

An important outcome of higher order calculations is the Higgs boson  $p_T$  spectrum. At lowest order, the Higgs boson is produced with no transverse momentum. At higher orders in  $\alpha_s$ , the effects of soft and soft plus collinear gluon emission from the initial state partons are numerically significant. At low  $p_T$ , the usual factorization approximation fails and large logarithms of the form  $\alpha_s^n \log^m(M_h^2/p_T^2)$  appear. These large logarithms can be

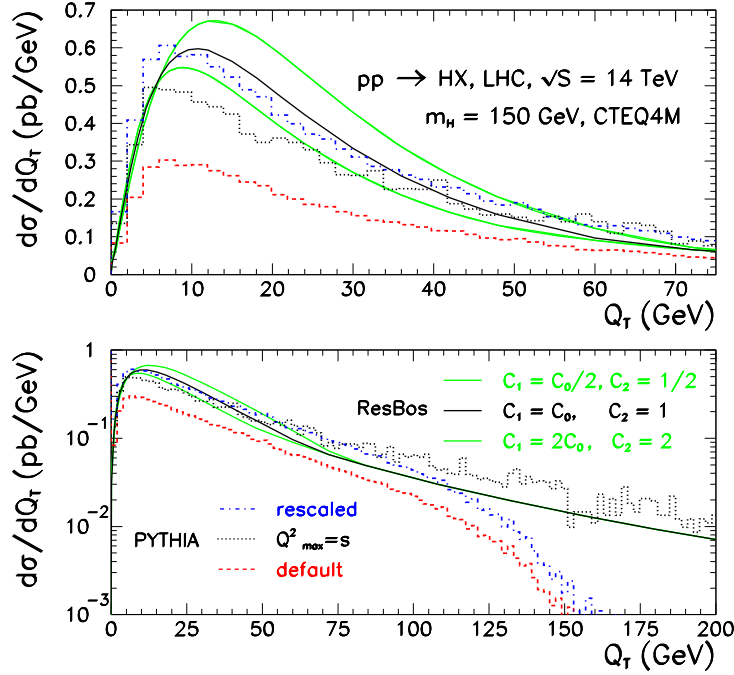


FIG. 5: Comparison of the Higgs  $p_T$  spectrum derived using soft gluon resummation at low  $p_T$ , matched with the exact calculation to  $\mathcal{O}(\alpha_s^3)$  at high  $p_T$  (solid), with PYTHIA (dashed). The 3 solid curves are estimates of the uncertainty from unknown NNLO contributions. From Ref. [8]

resummed to give a result which is valid at low  $p_T$ . At an intermediate value of  $p_T$ , the resummed form can be matched with the exact matrix element calculation to  $\mathcal{O}(\alpha_s^3)$ , valid at large  $p_T$ . This result is shown in Fig. 5. The three solid curves in this plot represent an attempt to estimate uncalculated NNLO contributions to the resummed result. Ref. [8] estimates a  $\pm 10\%$  uncertainty due to these unknown terms. When the complete NNLO calculation is available, it will be possible to remove much of this uncertainty.

Since experimental searches rely strongly on Monte Carlo programs, it is important to understand how soft gluon emission is included in these programs. Monte Carlo programs typically produce the Higgs  $p_T$  spectrum using parton showering, which correctly reproduces the spectrum at low  $p_T$ , but underestimates the rate at higher  $p_T$ , as can be seen in Fig. 5. The correct spectrum at high  $p_T$  (as determined from the exact matrix element calculation) can be obtained using PYTHIA by judiciously adjusting the arbitrary renormalization scale.[8]

The NLO rate for Higgs plus 1- jet production at the LHC has been computed in the  $M_t \rightarrow \infty$  limit.[9] The corrections increase the rate by a factor of 1.5 – 1.6 and are almost constant over a large range of  $M_h$ , rapidity, and  $p_T$ . As with inclusive Higgs production, the renormalization/factorization scale uncertainty is significantly reduced by the inclusion of the NLO contributions, although the residual uncertainty is still rather large,  $\sim \pm 20\%$ . The NLO QCD results for all of the 2- and 3- body Higgs decays have existed for some time and are conveniently implemented in the FORTRAN code HDECAY.[10] Fig. 4 shows the variation of the inclusive Higgs production cross section calculated to NLO multiplied by the NLO branching ratios to various channels as the renormalization scale,  $\mu$ , is varied from  $M_h/2 < \mu < 2M_h$ ,  $\alpha_s(M_Z)$  is varied within the LEP 1- $\sigma$  limit,  $.115 < \alpha_s(M_Z) < .123$  and  $m_b$  is varied within the particle data group range,  $4.5 \text{ GeV} < m_b(m_b) < 5 \text{ GeV}$ . The dominant source of uncertainty in the results of Fig. 4 is the renormalization/factorization scale dependence. By measuring combinations of final states, the uncertainty on the predictions can, however, be significantly reduced.[11] The theoretical uncertainty on the branching ratios alone is considerably smaller than on the product  $\sigma B$ . [12]

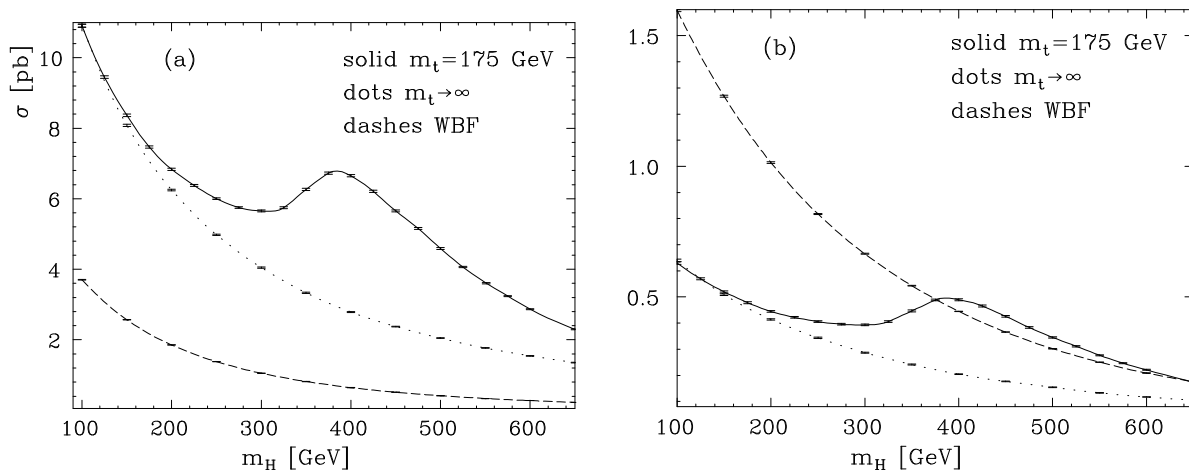


FIG. 6: (a)  $pp \rightarrow 2 \text{ jets} + h$  from the weak boson fusion sub-process at  $\sqrt{s} = 14 \text{ TeV}$  (dashed) and background from the  $gg \rightarrow ggh$  sub-process calculated exactly (solid) and in the  $M_t \rightarrow \infty$  limit (dotted). (b) Same as (a), but with cuts designed to enhance the weak boson fusion contribution. From Ref [14].

### B. Vector Boson Fusion

Vector boson fusion can be used to measure the  $WW_h$  and  $ZZ_h$  couplings at the LHC.[11] The NLO QCD corrections to  $pp \rightarrow 2\text{-jets} + h$  through the vector boson sub-process are quite small, [13] and the uncertainty on the production rate is estimated from the small scale dependence to be  $\sim 1 - 2\%$ .

It is necessary to separate the signal,  $qq \rightarrow qqh$  (which probes the  $WW_h$  and  $ZZ_h$  couplings), from the background,  $gg \rightarrow ggh$  (which depends only on the  $t\bar{t}h$  Yukawa coupling) and first enters at 1-loop.[14] Since the dominant contribution to the background arises from gluons in the initial state, the background is enhanced by the large gluon luminosity at the LHC. The  $gg \rightarrow ggh$  contribution to the Higgs plus 2-jet signal has been computed both in the  $M_t \rightarrow \infty$  limit and retaining the full  $M_t$  mass dependence and the results are shown in Fig. 6. The  $m_t \rightarrow \infty$  limit is a good approximation to the full result only for  $M_h < 2M_t$ . The weak boson fusion process produces well separated, forward jets, while the jets from the gluon fusion sub-process are more isotropic. Using cuts designed to enhance the vector boson fusion contribution, shown in Fig 6(b), it is clear that it will be possible to separate the gluon fusion sub-process from the vector boson fusion contribution for  $M_h < 2M_t$ . The weak boson fusion processes dominate over the gluon initiated processes by about a factor of 3 to 1 after applying the appropriate cuts and for  $M_h < 2M_t$ .

### C. Associated Production

A Higgs boson in the mass range around  $120 - 140 \text{ GeV}$  is particularly difficult to observe at the LHC since the preferred channel,  $h \rightarrow \gamma\gamma$ , suffers from a small rate and large backgrounds. In this region, the associated production channel,  $pp \rightarrow t\bar{t}h$ , may be useful to confirm an elusive Higgs signal. Although the production rates are small,  $\sim .5 - .8 \text{ pb}$ , the signature with the final state  $W^+W^-b\bar{b}b\bar{b}$  is spectacular. This process is of particular interest since it can be used to measure the  $t\bar{t}h$  Yukawa coupling.

The  $t\bar{t}h$  process proceeds predominantly through gluon fusion at the LHC. The complete NLO results have been found in Ref. [15] and are shown in Fig. 7. The NLO predictions show a significantly reduced scale dependence and increase the rate by roughly 20% from the LO predictions over the entire intermediate Higgs mass range.

## III. TEVATRON

Higgs boson production rates at the Tevatron are much smaller than at the LHC, but with the increased luminosity of Run II, it may be possible to observe a Higgs signal for a Higgs mass below around  $180 \text{ GeV}$ [16]. The dominant production mode is gluon fusion, with a cross section between  $1.0$  and  $0.2 \text{ pb}$  at  $\sqrt{s} = 2 \text{ TeV}$  for  $M_h$  in the  $120 - 180 \text{ GeV}$  region. Gluon fusion, however, suffers from large QCD backgrounds to the dominant  $h \rightarrow b\bar{b}$

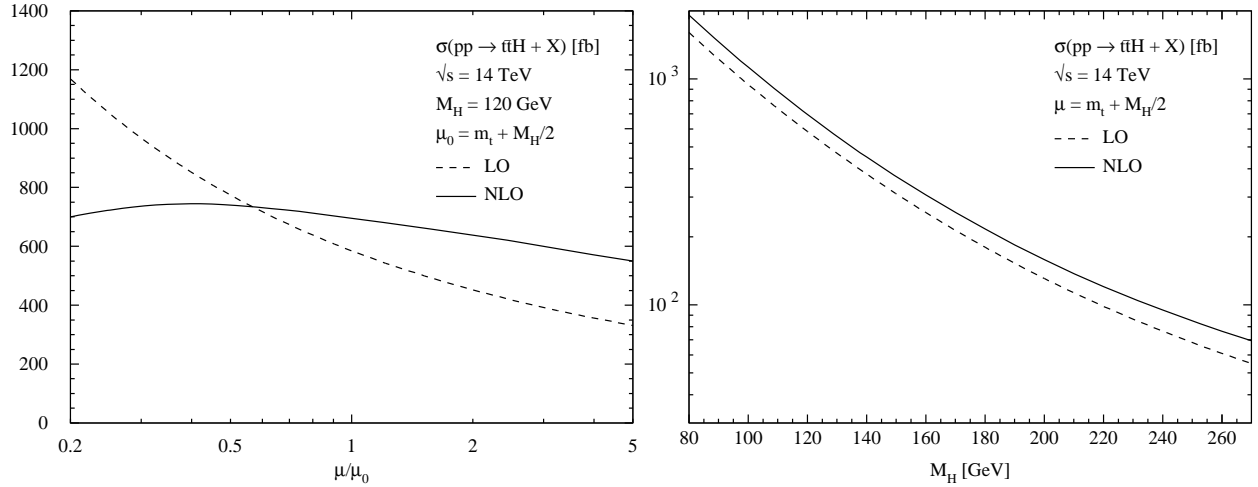


FIG. 7: (a) Dependence of  $\sigma_{LO,NLO}(p\bar{p} \rightarrow t\bar{t}h)$  on the renormalization/factorization scale  $\mu$ , at  $\sqrt{s} = 14 \text{ TeV}$ , for  $M_h = 120 \text{ GeV}$ . (b)  $\sigma_{NLO}$  and  $\sigma_{LO}$  for  $p\bar{p} \rightarrow t\bar{t}h$  as a function of  $M_h$ , at  $\sqrt{s} = 2 \text{ TeV}$ , for  $\mu = m_t$  and  $\mu = 2m_t$ . From Ref [15].

decay channel. The gluon fusion production mechanism may, however, be useful for  $140 < M_h < 180 \text{ GeV}$ , when combined with the  $h \rightarrow WW^*$  decay channel.

The most likely discovery channel at the Tevatron for  $M_h < 140 \text{ GeV}$  is the associated production of  $Wh$  or  $Zh$ , where an efficient trigger is provided by the leptonic decay modes of the vector bosons. For Higgs bosons in the  $M_h \sim 120 \text{ GeV}$  region, the associated production with a top quark pair may also be observable.[17] The status of the NLO QCD corrections to these processes is briefly discussed below and the rates at the Tevatron, including NLO QCD corrections for all channels, are shown in Fig. 8. (The rate for  $Zh$  production is about a factor of 2 below that for  $Wh$  production).

### A. Gluon Fusion

At the Tevatron, gluon fusion contributes roughly 65% of the total Higgs production cross section for  $120 \text{ GeV} < M_h < 180 \text{ GeV}$ . The NLO corrections to inclusive Higgs production are large and positive for all values of the Higgs mass. The NNLO corrections to  $gg \rightarrow h$  at the Tevatron have been computed by Harlander and Kilgore[3] and by Catani *et.al.*[4] in the soft plus collinear approximation described above and are shown in Fig. 3. Given the large numerical value of these partial corrections, a complete NNLO calculation is essential before reliable predictions can be made in this channel.

### B. Associated Production, $p\bar{p} \rightarrow Wh, Zh$

The  $Wh$  and  $Zh$  channels are the most promising discovery channels at the Tevatron for  $M_h < 140 \text{ GeV}$ . The NLO rate for  $p\bar{p} \rightarrow Wh$  is shown in Fig. 8 and is around  $.1 - .2 \text{ pb}$ . (This figure does not include the  $W$  and  $h$  decay branching ratios.) The NLO QCD corrections are the same as those for Drell-Yan and increase the rate by about 30% from the lowest order prediction.[18] The dependence of the NLO corrected rate on the choice of parton distribution functions is quite small, but there remains about a 12% uncertainty in the prediction due to the residual renormalization/factorization scale dependence.

Since the dominant decay of a Higgs boson below  $M_h \sim 140 \text{ GeV}$  is to  $b\bar{b}$  pairs, the irreducible background processes to  $p\bar{p} \rightarrow Wh$  and  $p\bar{p} \rightarrow Zh$  are  $p\bar{p} \rightarrow Wb\bar{b}$  and  $p\bar{p} \rightarrow Zb\bar{b}$ . These background processes have been calculated to NLO in Ref.[19] and the results implemented in the Monte Carlo program, MCFM. The NLO

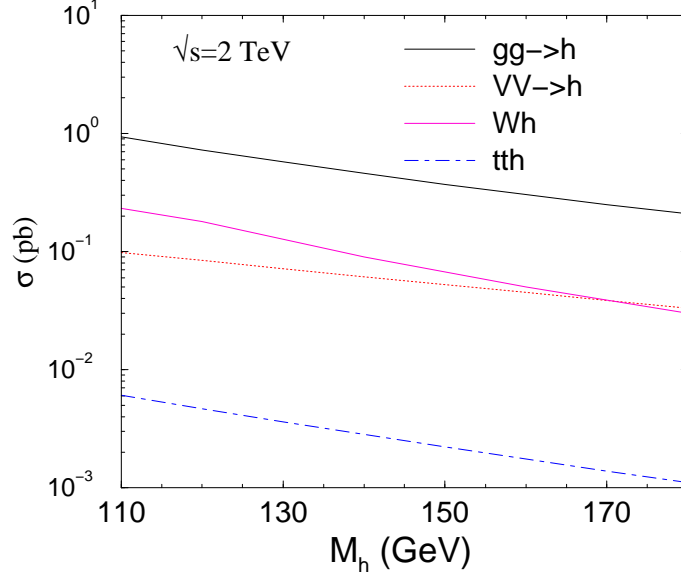


FIG. 8: NLO rates for Higgs production in  $p\bar{p}$  collisions at  $\sqrt{s} = 2 \text{ TeV}$ , evaluated at the renormalization/factorization scale  $\mu = M_h$ . (The process  $p\bar{p} \rightarrow t\bar{t}h$  is evaluated at  $\mu = 2m_t$ ).

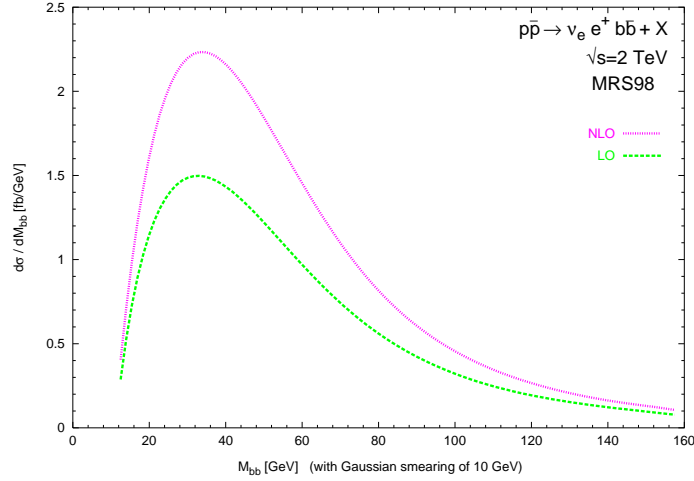


FIG. 9: The  $m_{b\bar{b}}$  distribution of the  $W^+(\rightarrow \nu_e e^+) b\bar{b}$  background to the Higgs signal, ( $p\bar{p} \rightarrow Wh$ ), at LO and NLO at  $\sqrt{s} = 2 \text{ TeV}$ . The  $b$ -quark tagging efficiency is not included. From Ref. [19].

corrections are large and positive and change the shape of the  $b\bar{b}$  distribution near the peak, as can be seen in Fig. 9. The  $K$  factors for the background  $Wb\bar{b}$  and  $Zb\bar{b}$  processes are larger than those for the  $Wh$  and  $Zh$  signals and have not been included in the studies of Ref. [19].

### C. Associated Production, $p\bar{p} \rightarrow t\bar{t}h$

At the Tevatron, the associated production of  $t\bar{t}h$  proceeds primarily through  $q\bar{q}$  annihilation. While the rate for  $t\bar{t}h$  production is small, the signature is distinctive. Unlike at the LHC, at the Tevatron the invariant mass distributions of the final state  $b\bar{b}$  pairs from the  $t\bar{t}h$  signal have rather a different shapes from the background



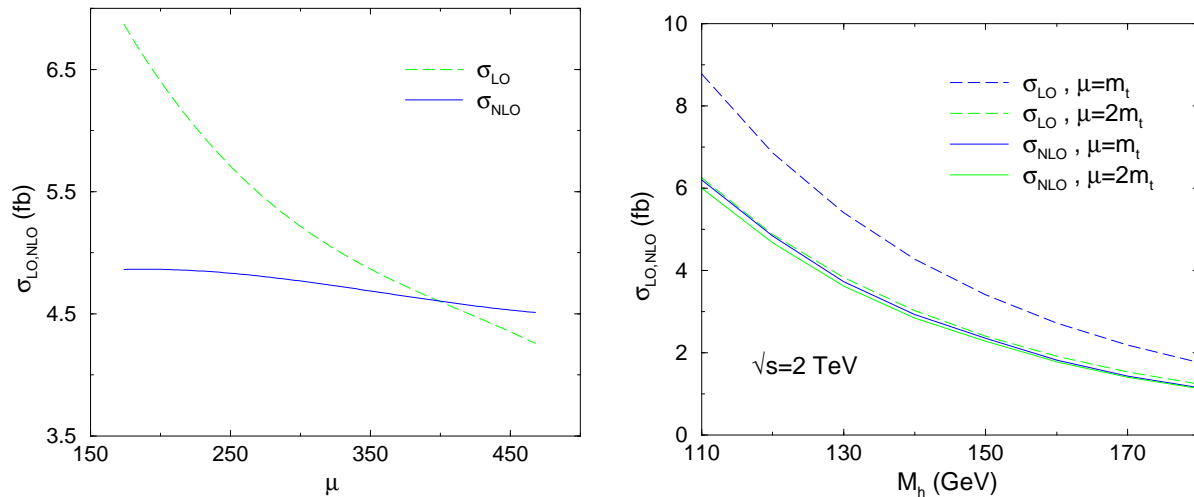


FIG. 10: (a) Dependence of  $\sigma_{LO,NLO}(p\bar{p} \rightarrow t\bar{t}h)$  on the renormalization/factorization scale  $\mu$ , at  $\sqrt{s} = 2$  TeV, for  $M_h = 120$  GeV. (b)  $\sigma_{NLO}$  and  $\sigma_{LO}$  for  $p\bar{p} \rightarrow t\bar{t}h$  as a function of  $M_h$ , at  $\sqrt{s} = 2$  TeV for  $\mu = M_t$  and  $\mu = 2M_t$ . From Ref [20].

and preliminary studies suggest that it may be possible to observe this channel at the Tevatron.[17]

The next to leading order results have been computed recently by two groups, with excellent agreement.[15, 20] The NLO result shows a reduced scale dependence from the lowest order result and a slightly reduced cross section from the lowest order prediction. For example, for  $M_h = 120$  GeV and  $\mu = M_t$ , the NLO total cross section is reduced to  $4.86 \pm 0.03$  fb from the lowest order prediction of  $6.868 \pm .002$  fb. The reduction is much less dramatic at  $\mu = 2M_t$ , as can be seen from Fig. 10. Only for renormalization/factorization scales larger around than  $\mu = 2M_t + M_h$  is the NLO cross section larger than the lowest order rate. Combining the residual scale dependence with the error from the parton distribution functions ( $\sim 6\%$ ) and from  $m_t$  (7%), we estimate the uncertainty on the theoretical prediction as about 12%.

#### IV. CONCLUSIONS

NLO corrections to all Higgs production channels of interest at hadron colliders have now been completed. These NLO predictions show a significantly reduced renormalization/factorization scale dependence from the LO predictions, leading to increased confidence in the validity of the predictions. Complete NNLO corrected rates for inclusive Higgs production should be available soon. Consistent NNLO calculations will, however, require structure functions derived to NNLO, which are not yet available.

#### Acknowledgments

I thank my collaborators, Laura Reina and Doreen Wackerroth, for many valuable discussions. This work is supported by the U.S. Department of Energy under grant DE-AC02-76CH00016.

- 
- [1] See, for example, ATLAS Detector and Physics Performance Technical Design Report, LHCC99-14/15.
  - [2] M. Spira *et. al.*, *Nucl. Phys.* **B453** (1995) 17; S. Dawson, *Nucl. Phys.* **B359** (1991) 283.
  - [3] R. Harlander and W. Kilgore, Snowmass proceedings, hep-ph/0110200; *Phys. Rev.* **D64** (2001) 013015.
  - [4] S. Catani, D. de Florian, and M. Grazzini, *JHEP* **0105** (2001) 025.
  - [5] R. Harlander, *Phys. Lett.* **B492** (2000) 74.
  - [6] M. Kramer, E. Laenen, and M. Spira, *Nucl. Phys.* **B511** (1998) 523.
  - [7] A. D. Martin *et. al.*, *Eur. Phys. Jour.* **C18** (2000) 117; W. van Neerven and A. Vogt, *Phys. Lett.* **B490** (2000) 111, *Nucl. Phys.* **B588** (2000) 345.
  - [8] C. Balazs, hep-ph/0008169, C. Balazs, J. Huston, and I. Puljak, *Phys. Rev.* **D63** (2001) 014021.
  - [9] D. de Florian, M. Grazzini, and Z. Kunszt, *Phys. Rev. Lett.* **82** (1999) 5209.

- [10] M. Spira, *Comput. Phys. Commun.* **108** (1998) 56.
- [11] D. Zeppenfeld *et. al.*, *Phys. Rev.* **D62** (2000) 010309; hep-ph/0005151.
- [12] M. Battaglia and K. Desch, hep-ph/0101165.
- [13] T. Han, G. Valencia, and S. Willenbrock, *Phys. Rev. Lett.* (1992) 3274.
- [14] V. Del Duca *et. al.*, hep-ph/0109147; hep-ph/0108030; hep-ph/0105129.
- [15] W. Beenacker *et. al.*, *Phys. Rev. Lett.* **87** (2001) 201805.
- [16] M. Carena *et. al.*, “Report of the Higgs Working Group”, hep-ph/0010338.
- [17] J. Goldstein *et. al.*, *Phys. Rev. Lett.* **86** (2001) 1694.
- [18] T. Han and S. Willenbrock, *Phys. Lett.* **B273** (1991) 167.
- [19] R. K. Ellis and S. Veseli, *Phys. Rev.* **D60** (1999) 011501; J. Campbell, hep-ph/0105226.
- [20] L. Reina and S. Dawson, *Phys. Rev. Lett.* **87** (2001) 201804; L. Reina, S. Dawson, and D. Wackeroth, hep-ph/0109066, hep-ph/0110299.